

AN ITERATIVE ENHANCEMENT OF HIGHER ORDER NONLINEAR MIXTURE MODEL FOR ACCURATE HYPERSPECTRAL UNMIXING

Andrea Marinoni¹, Javier Plaza², Antonio Plaza² and Paolo Gamba¹

¹Dipartimento di Ingegneria Industriale e dell'Informazione, Università degli Studi di Pavia, Pavia, Italy.

E-mail: {andrea.marinoni, paolo.gamba}@unipv.it

²Hyperspectral Computing Laboratory, University of Extremadura, Cáceres, Spain.

E-mail: {jplaza, aplaza}@unex.es

ABSTRACT

In order to provide a careful description of the interactions among endmembers in hyperspectral images, a new method for adaptive design of mixture models for hyperspectral unmixing is introduced. Specifically, the proposed approach relies on exploiting geometrical features of hyperspectral signatures in terms of nonorthogonal projections onto the space induced by the endmembers' spectra. Then, an iterative process is deployed in order to understand the order of local nonlinearity that is displayed by each endmember over every pixel. Experimental results show that the proposed approach is actually able to retrieve thorough information on the nature of the nonlinear effects over the image while providing excellent performance in reconstructing the given dataset.

Index Terms— Nonlinear hyperspectral unmixing, adaptive fitting, iterative nonlinearity detection, nonorthogonal projection

1. INTRODUCTION

Accurately estimating the elements in Earth observations is crucial when assessing specific features such as air quality index, water pollution estimate and urbanization process behavior. Moreover, physical-chemical composition can be retrieved from hyperspectral images when proper unmixing architectures are employed [1]. Specifically, when linear and nonlinear combinations of endmembers are accurately characterized, hyperspectral unmixing plays a key-role in understanding and quantifying phenomena occurring over the instantaneous field-of-view (IFOV). Thus, reliable detection of nonlinear reflectance behavior can play a key-role in enhancing hyperspectral unmixing performance. Several papers have recently addressed the topic of nonlinearity detection in hyperspectral images. For instance, a posteriori statistical tests have been used to understand bilinearity [2], [3], [4]. In [1], a semi-supervised approach to address the higher order nonlinearity detection issue has been proposed. Indeed, a framework for efficient p -linear unmixing that considers a pre-processing step to estimate the nonlinearity order of

each pixel is introduced. Hence, an artificial neural network (ANN) is properly trained and set to perform a reliable estimation of the order of the nonlinear interactions that occur over every pixel of the hyperspectral scene. This architecture delivers an effective improvement in hyperspectral unmixing performance, as it prevents overfitting effects to impact onto the characterization process.

Although the aforementioned methods might actually provide enhancement in understanding and quantifying the nonlinear reflectance interactions, computational complexity still represents an issue for actual implementation and development of those algorithms. Further, they do not avoid the occurrence of local overfitting that is delivered by inaccuracy in determining the order of the nonlinearity each endmember is involved in. Hence, efficient methods that aim to face the nonlinearity detection issue within hyperspectral images must be based onto new strategies, which can actually deliver solid improvements in spectral unmixing. In this paper, a new method for adaptive design of mixture models for hyperspectral unmixing is introduced. Specifically, the proposed approach relies on exploiting geometrical features of hyperspectral signatures in terms of nonorthogonal projections onto the space induced by the endmembers' spectra. Then, an iterative process is deployed in order to understand the order of local nonlinearity that is displayed by each endmember over every pixel. Experimental results show that the proposed approach is actually able to retrieve thorough information on the nature of the nonlinear effects over the image while providing excellent performance in reconstructing the given dataset. The paper is organized as follows. Section 2 describes the proposed method. Section 3 describes the experimental results. Finally, Section 4 concludes with some final remarks.

2. METHODS

Let $\underline{Y} = \{y_l\}_{l=1,\dots,P}$ be a P -pixel image, where $y_l = [y_{l_n}]_{n=1,\dots,N}$ is the N -band spectral signature of the l -th pixel. Then, let $\mathcal{M} = \{m_r\}_{r=1,\dots,R}$ be the set of the end-

members that can be drawn over \underline{Y} according to an endmember extraction algorithm (EEA). Moreover, let us consider the fully constrained least squares (FCLS) [5] optimization algorithm in order to unmix the given image. Hence, when we run FCLS over the l -th pixel considering the endmember spectra in \mathcal{M} , we obtain

$$\underline{y}_l = \hat{\underline{y}}_l^{(L)} + \hat{\underline{n}} = \sum_{r=1}^R \hat{a}_{lr} \underline{m}_r + \hat{\underline{n}}, \quad (1)$$

where $\hat{a}_{lr} = [\hat{a}_{lr}]_{r=1, \dots, R}$ are the coefficients that drive the linear mixture as estimated by the FCLS, i.e., $\sum_{r=1}^R \hat{a}_{lr} = 1$ and $\hat{a}_{lr} \geq 0 \forall r$. Moreover, $\hat{\underline{n}}$ is the noise residual that results from the FCLS linear unmixing. Hence, we can consider $\hat{\underline{y}}_l^{(L)}$ as the best linear approximation of \underline{y}_l when we employ FCLS unmixing as driven by the endmember spectra.

Let us consider now the set $\mathcal{M}'^{(2)}$ of the spectral signatures provided by the extracted endmembers and their second-order combinations, i.e., $\mathcal{M}' = \mathcal{M} \cup \mathcal{M}'^{(2)}$, where $\mathcal{M}'^{(2)} = \{\mathcal{M}_{r'}^{(2)} = \underline{m}_{r'}^2\}_{r'=1, \dots, R}$ where $\underline{m}_{r'}^2 = \underline{m}_{r'} \odot \underline{m}_{r'}$. Thus, when we run FCLS according to the \mathcal{M}' set of endmembers, we obtain the following equation:

$$\underline{y}_l = \hat{\underline{y}}_l^{(L)} + \hat{\underline{y}}_l^{(NL)} + \hat{\underline{n}}' = \sum_{r=1}^R \hat{a}'_{lr} \underline{m}_r + \sum_{r'=1}^R \hat{\beta}'_{lr'} \underline{m}_{r'}^2 + \hat{\underline{n}}', \quad (2)$$

where $\hat{a}'_{lr} = [\hat{a}'_{lr}]_{r=1, \dots, R}$ and $\hat{\beta}'_{lr'} = [\hat{\beta}'_{lr'}]_{r'=1, \dots, R}$ are the coefficients that drive the linear and bilinear mixture as estimated by the FCLS, respectively, i.e., $\sum_{r=1}^R \hat{a}'_{lr} + \sum_{r'=1}^R \hat{\beta}'_{lr'} = 1$, $\hat{a}'_{lr} \geq 0 \forall r$, $\hat{\beta}'_{lr'} \geq 0 \forall r'$. Moreover, $\hat{\underline{n}}'$ is the noise residual that results when FCLS unmixing is fed by the \mathcal{M}' set of endmembers. Let us now assume that the l -th pixel results from a linear combination of the endmember spectra in \mathcal{M} , i.e., $\underline{y}_l = \sum_{r=1}^R a_{lr} \underline{m}_r + \underline{n}$, where \underline{n} represents the noise delivered by acquisition system. In that case, the following equation holds: $\lim_{\|\underline{n}\|^2 \downarrow 0} \|\hat{\underline{y}}_l^{(L)} - \underline{y}_l^{(L)}\|^2 = 0$. In other words, when the l -th pixel represents a linear mixture of the R endmembers in the scene, the contribution provided by $\hat{\underline{y}}_l^{(NL)}$ in (2) is negligible. Therefore, if we are interested in understanding whether the l -th pixel can be considered as a result of a linear combinations of reflectances, in the ideal case (i.e., when the pixel noise is not relevant), we can just compute the Euclidean distance between $\hat{\underline{y}}_l^{(L)}$ and $\underline{y}_l^{(L)}$ and call for a linear mixture on the l -th pixel if it is equal to zero.

On the other hand, if the target pixel spectrum results from a nonlinear combination of endmembers, the aforesaid property does not hold anymore. Indeed, let us consider the mismatch between the linear contributions in (1) and (2), i.e., $\hat{\underline{y}}_l^{(L)} - \underline{y}_l^{(L)} = \hat{\underline{\delta}} = \sum_{r=1}^R \hat{\delta}_r \underline{m}_r$, where $\hat{\delta}_r = \hat{a}_{lr} - \hat{a}'_{lr}$. Thus, in order to retrieve a reliable and efficient metric for understanding and quantifying the effective nonlinear contribution provided by each endmember to the l -th pixel mixture, we

can consider the displacement between $\hat{\underline{y}}_l^{(L)}$ and $\underline{y}_l^{(L)}$ from a geometrical point of view.

Further, by considering (1) and (2), the following equation holds:

$$\hat{\underline{\delta}} = \hat{\underline{y}}_l^{(NL)} + \underline{\delta}_n = \hat{\underline{y}}_l^{(NL)} + (\hat{\underline{n}}' - \hat{\underline{n}}). \quad (3)$$

Therefore, we can assume that if the most of the $\hat{\underline{\delta}}$ displacement is collected by the nonlinear contributions in $\hat{\underline{y}}_l^{(NL)}$, then the l -th pixel might represent a nonlinear combination of the endmembers in the scene. On the other hand, if the $\hat{\underline{\delta}}$ difference is mostly delivered by the noise residual difference in $\underline{\delta}_n = \hat{\underline{n}}' - \hat{\underline{n}}$, then we can assume that the nonlinear contributions as estimated by FCLS can be considered as negligible, s.t. the mixture provided by l -th pixel is carried by the linear combinations of the endmember spectra.

Moreover, let us take a look to the local contributions carried by each endmember to the reconstructed spectral signature after FCLS unmixing as in (2). If we apply the aforementioned rule to the local scale, we can assume that a given endmember is not involved in any nonlinear spectral mixture within the target pixel signature as long as the major amount of the displacement in $\hat{\underline{\delta}}$ is collected by the $\underline{\delta}_n$ projection onto the direction marked by the given endmember itself. Further, if we iterate this process for investigating several nonlinearity orders, we can retrieve a new criterion for identifying the best approximating polynomial mixture model for the given hyperspectral signature.

Hence, in order to design a reliable overall metric of this effect, we must define a measure on which we could obtain coherent and thorough estimates and evaluations on the behavior of the displacements in (3). In that sense, the quantities in (3) must be referred to a mutual vectorial field, s.t. distance and difference definitions can be delivered according to Euclidean geometry [6]. Thus, in order to deliver this new common environment for the signatures in (3), we might need to consider every quantity in (3) as an object in another space where likelihoods can be safely computed according to Euclidean distances geometry [6].

In that sense, considering the subspace induced by the endmember signatures in \mathcal{M} might help to achieve a thorough improvement in terms of reliability and accuracy of the investigation. Specifically, reducing the N -dimensional space to the \mathcal{M} subspace induces a hull where each endmember spectrum represents one of the basis. Therefore, as $|\underline{m}_r \cdot \underline{m}_s| \geq 0 \forall \underline{m}_r, \underline{m}_s \in \mathcal{M}$, it is possible to achieve a close set where Euclidean geometry applies [6].

Indeed, as $\hat{\underline{\delta}}$ is defined as a weighted sum on the endmembers in \mathcal{M} , we can consider $\hat{\delta}_r$ as the projection of the displacement $\hat{\underline{a}}_l - \underline{a}'_l$ onto the basis of the \mathcal{M} -induced subspace as determined by the r -th endmember. Thus, in order to obtain a coherent computation for volume comparison onto a consistent domain, it is necessary to evaluate the contribution

provided by $\hat{y}'_l^{(NL)}$ and $\hat{\delta}_n$ onto each endmember basis of the \mathcal{M} vectorial field [6], i.e., we can rewrite (3) as follows:

$$\hat{\underline{d}} = \sum_{r=1}^R \hat{\delta}_r \underline{m}_r = \sum_{r=1}^R \pi_r(\hat{y}'_l^{(NL)}) \underline{m}_r + \sum_{r=1}^R \pi_r(\hat{\delta}_n) \underline{m}_r, \quad (4)$$

where $\pi_r(\underline{z})$ identifies the nonorthogonal projection of \underline{z} onto the direction imposed by the r -th endmember. Hence, (4) provides a coherent and consistent representation of each term in (3) onto the common domain delivered by the \mathcal{M} -induced subspace. Actually, as typically the endmembers in \mathcal{M} are not perfectly orthogonal to each other, the computation of the π_r coefficients in (4) can not be performed according to orthogonal projection algorithms. Thus, in order to obtain the accurate estimation of each π_r , we can write a proper system of linear equations in order to take advantage of the properties of Clifford algebra [6]. Specifically, let us consider a N -element array \underline{z} as defined as $\underline{z} = \sum_{r=1}^R \pi_r(\underline{z}) \underline{m}_r$. Then, let us consider R linear equations obtained from the aforementioned representation of \underline{z} by considering the inner product of every term onto an endmember, i.e., the i -th linear equation would be written as $\underline{z} \cdot \underline{m}_i = \sum_{r=1}^R \pi_r(\underline{z}) \underline{m}_r \cdot \underline{m}_i$. Hence, we can write the whole system in matrix form as $\underline{A}_{\mathcal{M}} \times \underline{\pi}(\underline{z})^T = \underline{b}^T$, where $\underline{A}_{\mathcal{M}} = \{A_{\mathcal{M}_{jk}}\}_{(j,k) \in \{1, \dots, R\}^2}$, $A_{\mathcal{M}_{jk}} = \underline{m}_j \cdot \underline{m}_k$, $\underline{\pi}(\underline{z}) = [\pi_i(\underline{z})]_{i=1, \dots, R}$, $\underline{b} = [b_i]_{i=1, \dots, R}$, $b_i = \underline{z} \cdot \underline{m}_i$.

Then, we can use Cramer's rule in order to retrieve the elements in $\underline{\pi}(\underline{z})$ [6]. Specifically, let us consider $\underline{A}_{\mathcal{M}} = [A_{\mathcal{M}_1} | \dots | A_{\mathcal{M}_j} | \dots | A_{\mathcal{M}_R}]$, where $A_{\mathcal{M}_j}$ identifies the j -th column of $\underline{A}_{\mathcal{M}}$. Thus, let us define $\underline{A}_{\mathcal{M}}^{(h)}$ as the matrix that we obtain by replacing the h -th column of $\underline{A}_{\mathcal{M}}$ with \underline{b}^T , i.e., $\underline{A}_{\mathcal{M}}^{(h)} = [A_{\mathcal{M}_1} | \dots | A_{\mathcal{M}_{h-1}} | \underline{b}^T | A_{\mathcal{M}_{h+1}} | \dots | A_{\mathcal{M}_R}]$. Hence, by Cramer's rule, it is possible to state:

$$\pi_h(\underline{z}) = \det[\underline{A}_{\mathcal{M}}^{(h)}] \cdot (\det[\underline{A}_{\mathcal{M}}])^{-1}. \quad (5)$$

Therefore, we can obtain the nonorthogonal projections in (4) by operating on matrices induced by inner products in the endmembers' space. Once the $\underline{\pi}(\underline{z})$ coefficients are computed, the terms in (3) are mapped onto a coherent space. Hence, it is possible to retrieve local contributions of each endmember to the nonlinear mixture in the target pixel spectrum by considering the distance of each corresponding element in the three terms of (4). Then, to consider the local contribution provided to the nonlinearity of the system by each endmember we have to take into account the corresponding nonorthogonal projections delivered by $\hat{y}'_l^{(NL)}$ and $\hat{\delta}_n$. Indeed, once the spectral signatures are represented as elements in the space induced by the endmembers, we can compare coherent quantities deployed over the directions of the new space bases. Specifically, if we compute the distances of the projections over the r -th endmember direction delivered by $\hat{y}'_l^{(NL)}$ and $\hat{\delta}_n$ to $\hat{\delta}_r$, we can recover a reliable likelihood of

the r -th endmember to be involved in nonlinear combinations collected in the target spectral signature. I.e., let us define $\Delta_r = |\hat{\delta}_r - \pi_r(\hat{y}'_l^{(NL)})| - |\hat{\delta}_r - \pi_r(\hat{\delta}_n)|$. Thus, we can assume that the r -th endmember is involved in the second order nonlinear effects that gathered in \underline{y}_l if $\Delta_r < 0$.

It is possible to notice that the aforementioned scheme is able to retrieve information on the bilinear effects delivered by the endmembers in \mathcal{M} since it relies on the nonlinear unmixing representation in (2). Specifically, $\hat{y}'_l^{(NL)}$ and $\hat{\delta}_n$ result from unmixing \underline{y}_l using the endmembers in $\mathcal{M}' = \mathcal{M} \cup \mathcal{M}^{(2)}$. However, if we aim at acquiring information on the actual order of the nonlinear effects that are driven by each endmember, we can iterate the proposed approach by extending \mathcal{M}' with the higher order contributions of the endmembers for which $\Delta_r < 0$. The general extension of this approach would turn into setting \mathcal{M}' at the k -th step of the process to $\mathcal{M}' \cup \overline{\mathcal{M}}^{(k)}$, where $\overline{\mathcal{M}}^{(k)}$ collects the k -linear contribution of the endmembers that have been considered as involved in the nonlinear effects at the $(k-1)$ -th step, i.e., those for which $\Delta_r < 0$ at the $(k-1)$ -th step. This process would iterate until $\Delta_r > 0 \forall r$. Hence, the hyperspectral mixture model that would result from this procedure might represent an instance of a multiple p -linear mixture model (mpLMM), as the nonlinearity order of each endmember contribution is set independently, i.e., (2) would turn at the end of the process into the following equation:

$$\underline{y}_l = \sum_{r=1}^R \hat{a}'_{lr} \underline{m}_r + \sum_{r'=1}^R \sum_{k'=2}^{p_{lr'}} \hat{\beta}'_{lr'k'} \underline{m}_{r'}^{k'} + \hat{n}', \quad (6)$$

where $p_{lr'}$ identifies the order of the r' -th endmember's contribution to the nonlinear mixture of the l -th pixel. Thus, the proposed method aims at leveraging the computational cost by focusing only on the endmembers that are estimated to be involved in the nonlinear effects that are recorded in the target pixel signature. Moreover, by adapting the nonlinearity order of each endmember share, the aforementioned framework aims at providing a careful description of the mixture combinations that occur onto the given IFOV. The next Section reports the performance in detecting the pixels that result from linear mixtures on the given hyperspectral scene as achieved by the aforementioned method.

3. EXPERIMENTAL RESULTS

We tested the new unmixing technique using an image over the World Trade Center area in New York City (Fig. 1(a)), collected by the AVIRIS instrument on 16 September 2001, just 5 days after the terrorist attacks that collapsed the two main towers and other buildings in the WTC area. The full data set considered consists on 614×507 pixels, with $N = 224$ bands and a spatial resolution of 1.7 m/pixel. Fig. 1(a)

shows a false color composite of the area using the 1.682, 1.107 and 655 nm channels, displayed as red, green and blue respectively. Extensive reference information, collected by the U.S. Geological Survey (USGS), is available for the WTC scene. Ten endmembers of the WTC scene have been extracted using the orthogonal subspace projection (OSP) algorithm [7].

Fig. 1(b) reports the reconstruction error (RE) performance as provided over the WTC image by the polytope decomposition (POD) method, ANN+POD architecture [1] and the proposed algorithm based on mpLMM. Specifically, POD have been used when the hyperspectral mixture is modeled by means of a 5-linear mixture model. On the other hand, the nonlinearity order used to unmix each pixel according to the ANN+POD scheme is set as in Fig. 2(a). Finally, Fig. 2(b), (c) and (d) report the nonlinearity orders of three endmembers over each pixel as estimated by means of the proposed approach. Moreover, the maximum value of nonlinearity that has been discovered by the proposed framework is 5. RE results show how the proposed approach is actually able to outperform the other higher order nonlinear hyperspectral unmixing architectures that have been introduced in [1]. Apparently, the proposed algorithm is actually able to detect the nonlinearities over the image. Moreover, the proposed method aims at avoiding the local overfitting provided by the p -linear mixture model when an higher nonlinearity order is applied to endmembers that poorly contribute to the overall nonlinear combinations which occur over each pixel (see Fig. 2). Thus, the proposed approach can be actually used for enhancing higher order nonlinear hyperspectral unmixing by an accurate detection of the nature of the reflectance combinations occurring over the considered image.

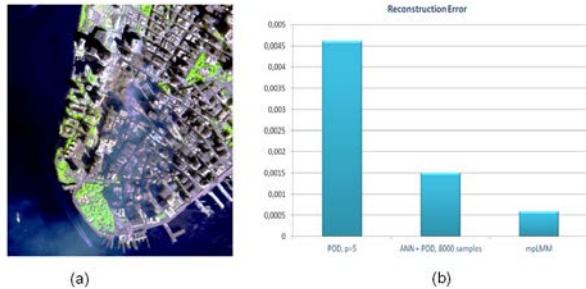


Fig. 1. (a): RGB composite of the WTC image. (b): reconstruction error performance as delivered by the polytope decomposition (POD) method, the ANN+POD architecture [1] and the proposed approach based on multiple p -linear mixture model (mpLMM).

4. CONCLUSION

A novel iterative method for designing mixture models for hyperspectral unmixing is introduced. The proposed approach

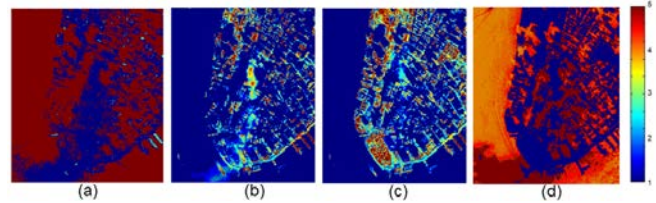


Fig. 2. (a): Nonlinearity order as estimated by the scheme in [1] on each pixel of the WTC image. (b), (c), (d): Nonlinearity orders estimated by the proposed method for three endmembers over the same image.

aims at understanding the the order of local nonlinearity that is displayed by each endmember over every pixel by projecting every quantity in the unmixing formula onto the space spanned by the given endmember set. Experimental results show that the proposed approach is actually able to retrieve thorough information on the nature of the nonlinear effects over the image while providing excellent performance in reconstructing the given dataset.

5. REFERENCES

- [1] A. Marinoni, J. Plaza, A. Plaza, and P. Gamba, “Nonlinear hyperspectral unmixing using nonlinearity order estimation and polytope decomposition,” *IEEE J. Sel. Top. App. Earth Obs. Rem. Sens.*, vol. 8, no. 6, pp. 2644–2654, June 2015.
- [2] Y. Altmann et al., “Nonlinearity detection in hyperspectral images using a polynomial post-nonlinear mixing model,” *IEEE Trans. on Image Proc.*, vol. 22, no. 4, pp. 1267–1274, Apr. 2013.
- [3] Y. Altmann et al., “Residual component analysis of hyperspectral images - application to joint nonlinear unmixing and nonlinearity detection,” *IEEE Trans. on Image Proc.*, vol. 23, no. 5, pp. 2148–2158, May 2014.
- [4] Y. Altmann et al., “Unsupervised post-nonlinear unmixing of hyperspectral images using a hamiltonian monte carlo algorithm,” *IEEE Trans. on Image Proc.*, vol. 23, no. 6, pp. 2663–2675, June 2014.
- [5] D. Heinz and C.-I. Chang, “Fully constrained least squares linear spectral mixture analysis method for material quantification in hyperspectral imagery,” *IEEE Trans. Geosci. Remote Sens.*, vol. 39, no. 3, pp. 529–545, Mar. 2001.
- [6] G.E. Bredon, *Topology and geometry*, Springer Verlag, 1993.
- [7] H. Ren and C.-I Chang, “Automatic spectral target recognition in hyperspectral imagery,” *IEEE Trans. Aerospace and Electron. Syst.*, vol. 39, no. 4, pp. 1232–1249, 2003.